



HAL
open science

An improved accelerated degradation model for LED reliability assessment with self-heating impacts

Minh-Tuan Truong, Phuc Do Van, Laurent Mendizabal, Benoît Iung

► To cite this version:

Minh-Tuan Truong, Phuc Do Van, Laurent Mendizabal, Benoît Iung. An improved accelerated degradation model for LED reliability assessment with self-heating impacts. *Microelectronics Reliability*, 2022, 128, pp.114428. 10.1016/j.microrel.2021.114428 . hal-03475747

HAL Id: hal-03475747

<https://hal.science/hal-03475747>

Submitted on 5 Jan 2024

HAL is a multi-disciplinary open access archive for the deposit and dissemination of scientific research documents, whether they are published or not. The documents may come from teaching and research institutions in France or abroad, or from public or private research centers.

L'archive ouverte pluridisciplinaire **HAL**, est destinée au dépôt et à la diffusion de documents scientifiques de niveau recherche, publiés ou non, émanant des établissements d'enseignement et de recherche français ou étrangers, des laboratoires publics ou privés.



Distributed under a Creative Commons Attribution - NonCommercial 4.0 International License

An improved accelerated degradation model for LED reliability assessment with self-heating impacts

Minh-Tuan Truong^{1,2}, Phuc Do^{1*}, Laurent Mendizabal² and Benoit Iung¹

¹Université de Lorraine, CRAN, UMR 7039, Campus Sciences, BP 70239, Vandoeuvre-les-Nancy, 54506, France

²Univ. Grenoble Alpes, CEA, Leti, F-38000 Grenoble, France

Abstract: Light-emitting diodes (LEDs) are a solid-state light source being used in numerous applications, including display, communications, medical services, etc. However, the reliability assessment of LED components is still challenging due to the growing up of the LED complexity and/or the miniaturization of assembly technologies. To face this challenge, this paper proposes a novel accelerated degradation testing (ADT) model considering the self-heating impact in the degradation process of a LED component. So, the self-heating impact is first analyzed and modeled. In fact, the junction temperature of a LED component depends not only on the heat generation (e.g., drive current, dispersing heat) but also on the current state (degradation level) of the component. Then, a modified stochastic difference equation is developed for modelling the degradation process by considering the self-heating impact. The LED reliability formulation is finally derived. In addition, an estimation method based on the maximum likelihood is developed to estimate the proposed model's parameters from experimental data. To validate our models, a case study for LED light sources is implemented. The obtained results show that, compared to the TM-21 standard and the conventional ADT methods, our proposed approach achieves better results in the LED reliability assessment.

Keywords: LED; reliability; degradation modelling; accelerated degradation testing; stochastic process

1 Introduction

Since the 2000s, Gallium nitrogen (GaN) light-emitting diodes (LEDs) have been widely used in multiple fields of application (e.g., display, communications, medical services, etc.) [1]. However, the growing complexity of LED technologies and the miniaturization of assembly technologies make harder for the industry and academic research to evaluate the reliability of the new LED products [2]. The direct consequence is that the reliability of these systems is more and more challenging to

*Corresponding author: phuc.do@univ-lorraine.fr

estimate. [Lumen degradation](#) is one of the main indicators of LED failure and has been studied in various works, see for instance [3, 4, 5, 6, 7, 8, 9, 10]. According to TM-21 standard [4], the LED's lifetime is evaluated, using an exponential law for modelling [lumen degradation](#), higher than 50.000h. Besides, stochastic processes, such as Wiener [5, 6] or gamma process [7, 9], at several accelerated conditions, are also used to model the LEDs' [lumen degradation](#). In both methods, thermal stress is one of the most commonly used methods to accelerate the failure/degradation of LED using the Arrhenius model, which describes the degradation rate of the [luminous intensity](#) of LED following the operational temperature [11]. In many studies, the junction temperature used in the Arrhenius model is considered to be constant and equal to the ambient temperature because it can be controlled with a temperature chamber during the acceleration test. However, it has been shown that the component's lifetime prediction, which used the ambient temperature to model the degradation rate, may lead to significant prediction errors and uncertainties with the actual application life [12].

Indeed, according to the literature, the junction temperature, which directly affects the LEDs' failures (e.g., semiconductor failure, interconnect failure), significantly influences on the degradation [2, 3, 13]. Thus, for the modelling of the LEDs' degradation rate, the junction temperature as thermal stress is more relevant than the ambient temperature in conventional ADT approaches. However, direct measurement of the junction temperature is complex and may lead to an important error [2, 14, 15]. Besides, based on LEDs' failure analyses (e.g., optical and infrared thermal microscopy, scanning electron microscope, etc.), many studies have shown that LED's junction temperature is not constant and may increase during the acceleration test due to the LED degradation impact [16, 12]. In addition, the increment of junction temperature may lead to further accelerate the LEDs' degradation rate [2, 13]. To sum up, due to the degradation impact, there is a loop of thermal stress, subjected to a self-heating on the LED component, which affects the LED degradation process over time. In that way, the self-heating phenomenon, shown through the increment of junction temperature, is an important issue and needs to be considered in the LEDs' degradation/failure modelling and reliability assessment. However, very few studies on this research topic are found in the literature [12].

To overcome this issue, this paper proposes a novel ADT model considering the self-heating phenomenon impacting the LED's degradation process. In that way, the self-heating impact is first analyzed and modelled mathematically. In fact, the junction temperature of a LED component depends not only on the heat generation (e.g., forward current, dispersing heat) but also on the current state (degradation level) of the component. Next, a modified stochastic difference equation (SDE) is developed for modelling and formulating the degradation process by considering the self-heating impact. The LED reliability formulation is then derived. To estimate the model's parameters from experimental data, an estimation method based on the maximum likelihood is also developed. This paper develops an extended version of the work presented in [17].

To describe the added value of our contributions, the rest of the paper is organized as follows:

we first introduce, in Section 2, the LED device used for our acceleration test. The failure and degradation behavior of the LED is then analyzed. In addition, the experimental platform is also presented. Next, the self-heating impact is mathematically modeled in Section 3. The degradation model and the reliability assessment considering the self-heating impact are formulated in Section 4. Furthermore, a maximum likelihood-based method for estimating the proposed model's parameters is also presented herein. Section 5 analyses some obtained results when applying the proposed model to our experimental dataset. Finally, the conclusions drawn from this work are presented in the last section.

Notations

IESNA	Illuminating Engineering Society of North America
LED	Light-emitting diode
ADT	Accelerated degradation test
SDE	Stochastic differential equation
FHT	First hitting time
PDF	Probability distribution function
CDF	Cumulative failure distribution function
MLE	Maximum likelihood estimate
DML	Discrete maximum likelihood
PCB	Printed circuit board
DL	Digital level

Abbreviations

E_a	Activation energy of component
k_B	Boltzmann constant
T_k	stress temperature at level k
n_k	Number of sample under stress level k
m_k	Number of measurement under stress level k
$\mu(\cdot)$	Degradation rate of component
D	Degradation failure threshold

2 Experiment description

In this section, we present the detail of an experiment for a LED in order to investigate the self-heating phenomenon, i.e., the increment of junction temperature due to the power dissipation and the LED degradation impact, and evaluate the LEDs' reliability. In that way, the LED studied, which was

chosen for the acceleration test, is firstly presented. Next, we present an experimental platform and the test condition. The failure and degradation behaviors are then analyzed based on the experimental dataset. In addition, the existence of an increment in junction temperature due to the degradation of the LED is also highlighted.

2.1 Device description and degradation characteristic

Device description In this study, gallium nitrogen (GaN) LED was chosen as the research object. The elementary structure consists of a GaN chip on the interconnected metal layer and the ceramic substrate soldered on an Aluminium (Al) support. Figure 1 presents an example of LED structure and its packaging on the printed circuit board (PCB). This is a LED Cree EZ1000, and it has a vertical structure with two topside $150 \times 150 \mu\text{m}$ square bond pad cathode (-) terminals and an 80:20 AuSn terminated anode (+) on the bottom of the silicon substrate [18]. The LED emitting layer is metallurgically bonded to the silicon substrate, and the periphery of the emitting mesa is passivated. These vertically structured, low forward voltage LED chips are approximately $170 \mu\text{m}$ in height.

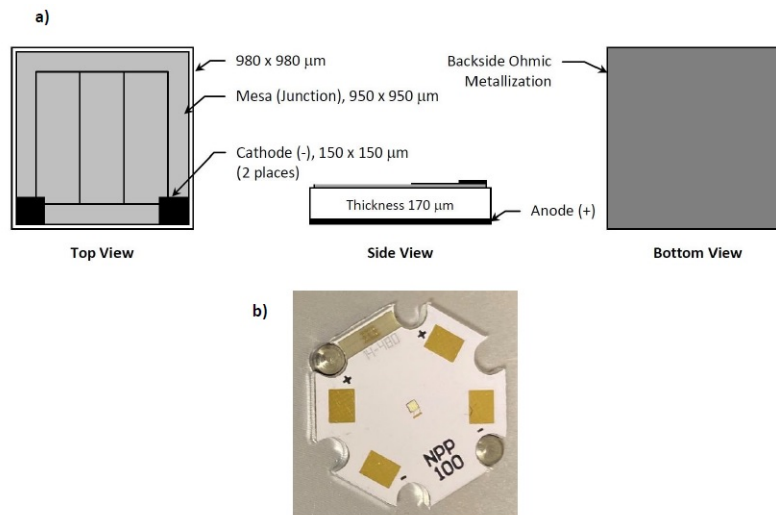


Figure 1: Details of LED Cree EZ10000; a) LEDs' structure diagram; b) LED packages on the PCB

It should be noticed that there is no encapsulant lens in the studied LED. Thus, there is no discolouration in the aged packages.

The failure of a LED is classified into open failure, short failure, and gradual degradation. The open and short failure is mainly due to electric shock or damage in the production process; however, the open and short failure rate is very small. While the gradual degradation mechanisms, which could come from the deterioration of the Ohmic contacts or/and semiconductor chips [2, 3, 8, 10, 13], affects significantly the LED failure. The previous studies revealed that gradual degradation of LED could suffer from gradual performance degradation, such as [lumen degradation](#) [2, 3]. It is shown that heat and current are two main causes of [lumen degradation](#), and they occur gradually over a long period

of operating time [2, 3, 8, 10].

Failure criteria The **luminous intensity** of a LED decreases when the LED degrades. A LED is considered as failed when its **luminous intensity** reaches a critical threshold. According to the Illuminating Engineering Society of North America (IESNA), the critical threshold for a LED is about 70% of the initial value of the **luminous intensity** of the LED, called L_{70} [4].

2.2 Experimental platform and test condition

Experimental platform: Figure 2 presents a global view of the experimental platform to characterize the LEDs' performance during the acceleration test. This system consists of a DC source meter, temperature chamber, and a spectrometer for optical measurement. In which:

- A KEITHLEY 2600 source meter generator is connected by an IEEE bus to the computer unit that controls the bench. This device is used as a bias current source and allows measuring the LED voltage.
- A spectrometer (USB2000+) is used to measure the spectral and intensity of LEDs.
- A climatic chamber (CLIMATS Excal) is used for thermal regulation during measurements and aging tests.
- An infrared camera (FLIR SC7000) is used to evaluate the LED temperature (LED surface temperature).

The infrared camera, which takes the image of LED surface, is a detector of indium antimony (InSb). However, these elements (e.g., GaN, substrate, wire bonds) have different emissivities, and each of them has its particular response to infrared. Thus, at a given temperature, all materials will be seen differently by the camera. Consequently, the camera must be calibrated before being used to estimate the LED temperature value accurately. Indeed, the calibrated camera is made as Figure 3. More details, we place the LED (non-powered) at three temperatures T_1 , T_2 and T_3 ($T_1 < T_3 < T_2$), then, the images are measured in units of digital levels (DLs) at these three temperature levels (i.e., $Im_1(i, j)$, $Im_2(i, j)$ and $Im_3(i, j)$ are the values provided by the pixel (i,j) at temperature T_1 , T_2 and T_3). The image given by the detector placed in front of a LED is therefore not uniform for all pixels due to technological dispersion and an optic presence that induces aberrations. Thus, it is necessary to bring the slope and offset all the pixels back to the average values. And, this three-point correction makes it possible to standardize the response of the pixels. After correction over the range of $23^{\circ}C - 90^{\circ}C$, all pixels provide the same output level.

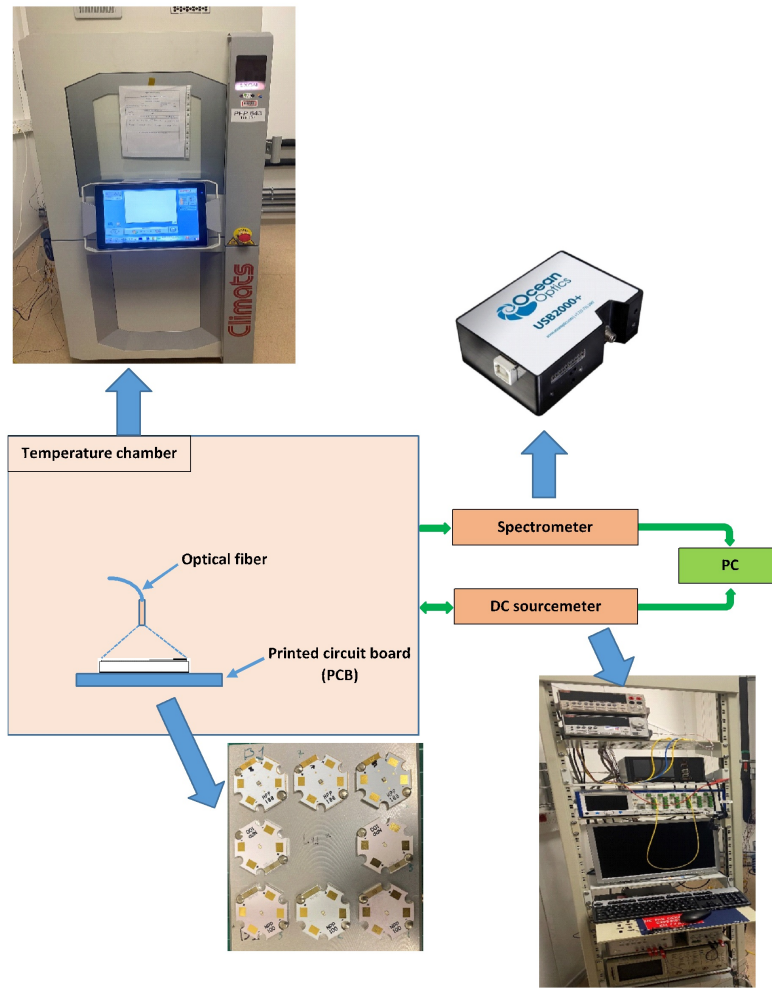


Figure 2: Global view of the experimental platform

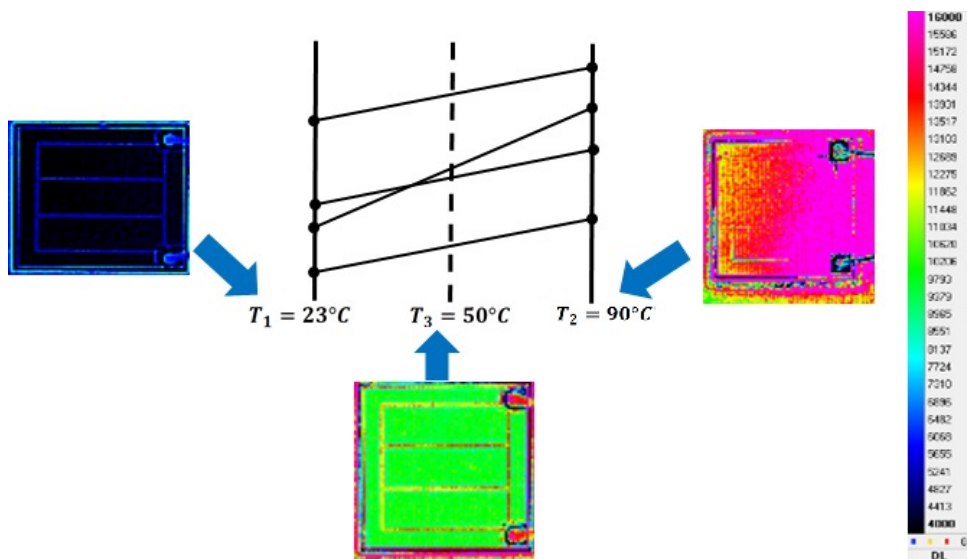


Figure 3: Representation of the pixel value as a function of temperature

After calibrating the camera, LED's temperature is calculated and analyzed from the thermal

image by using a proprietary software tool (Flir System Inc.). When observing a scene, an image ($Im(i, j)$) in units (DL) is recorded. The temperature of the scene observed by the pixel (i, j) of the matrix is given by [19]:

$$T_{frame}(i, j) = T_1 + (T_2 - T_1) \left[\frac{Im(i, j) - Im_1(i, j)}{Im_2(i, j) - Im_1(i, j)} \right] \quad (1)$$

Test condition: The choice of temperature condition, T_k with $k = 1, 2$, was determined based on the LED Cree EZ1000 data sheet [18]. The test condition of data used in this paper is shown in Table 1. In this case, the forward current is fixed at 350 mA for all tests.

Table 1: Test conditions

Terms	Test condition
Test duration	1.500 h
Data collection interval	Minimum of every 48h
Input current	350mA
Temperature	
T_1	$85^{\circ}C(358^{\circ}K)$
T_2	$100^{\circ}C(373^{\circ}K)$
Sample size	9 units under T_1 and 10 units under T_2

2.3 Preliminary analysis from experimental dataset

2.3.1 Evolution of the luminous intensity

Our experiment has been realized for 19 LEDs during 1500 hours with two test stress levels (9 LEDs with $T_1 = 85^{\circ}C$ and 10 LEDs with $T_2 = 100^{\circ}C$). The **luminous intensity**, denoted $P(t)$, was measured every 48 hours. To better show the evolution of the **luminous intensity** over time, we used the normalized **luminous intensity** ($P_{out}(t)$) that is defined as the ratio of the light output ($P(t)$) and its initial value $P(0)$. The obtained results are shown in Figure 4.

$$P_{out}(t) = \frac{P(t)}{P(0)} \quad (2)$$

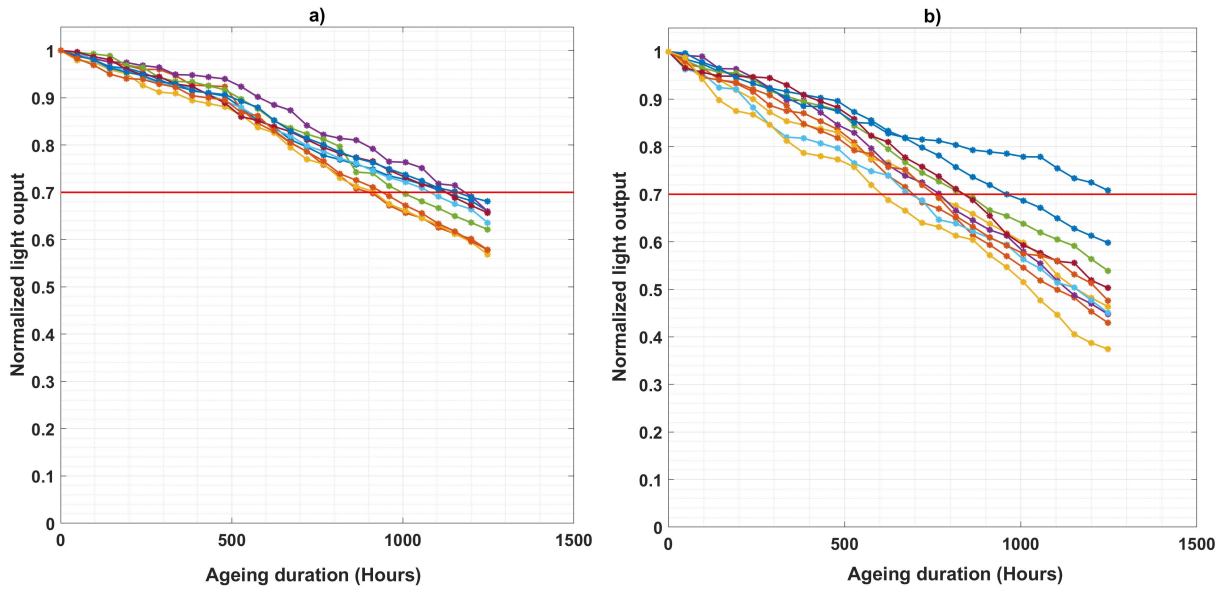


Figure 4: Lumen degradation at two stress conditions ; a) $T_1 = 85^{\circ}C$; b) $T_2 = 100^{\circ}C$

It is clear that under a stress temperature, the luminous intensity decreases with time, and the evolution of luminous intensity is not deterministic. Therefore, it is important to model this evolution in order to predict the failure time of the LED under a given stress temperature. In that way, a degradation model for the luminous intensity process is developed and presented in Section 4.

2.3.2 Impact of the forward current on the junction temperature

We analyze herein the variance of the LED's junction temperature using an infrared camera. Figure 5 shows the thermal image in units (DLs) taken before (Figure 5.a) and after applying the forward current of 350 mA (Figure 5.b). It is apparent that the forward current leads to a significant change (the area in the center of the image is brighter) in the thermal image due to the increment of the junction temperature of the LED. Indeed, this change is converted into the temperature increment by using Equation (1). Table 2 reports the results for 19 LEDs components in our experimentation.

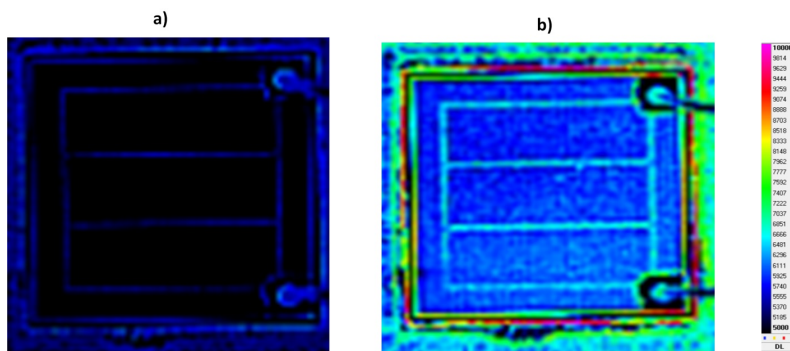


Figure 5: Thermal analysis of a LED: a) without forward current and b) with forward current at 350mA

Table 2: Increment of junction temperature due to the forward current

Component	ΔT [$^{\circ}C$]	Component	ΔT [$^{\circ}C$]
1	12.0	11	8.9
2	10.9	12	11.3
3	8.3	13	8.4
4	11.0	14	8.5
5	12.3	15	8.8
6	10.7	16	7.6
7	11.5	17	12.0
8	11.0	18	10.5
9	9.6	19	9.0
10	10.4		

Therefore, based on the obtained results, it is shown that an increment of junction temperature with an average of 10.14 degrees and a standard deviation of 1.14 degrees. Thus, with a 350 mA of forward current, the junction temperature becomes $95.14^{\circ}C$ and $110.14^{\circ}C$ when the stress condition of $85^{\circ}C$ and $100^{\circ}C$, respectively, are applied. The impact of the forward current on its junction temperature will be modeled and presented in the next section.

2.3.3 Impact of the lumen degradation on the junction temperature

Figure 6 shows the different images in units (DLs) provided by the infrared camera FLIR SC7000 at different time points t (before the acceleration test $t = 0$, $t = 576h$, $t = 720h$ and $t = 1500h$). It is shown that the junction temperature of LED increases during the acceleration test. Indeed, from these images, the increment on the LED junction temperature is evaluated by using the protocol presented in Section 2.2. The obtained results are reported in Table 3 and Table 4. It should be noticed that the increasing of the junction temperature may also affect the LED degradation process. Thus, there is herein a loop of thermal stress. The impact of the LED degradation on its junction temperature will be modeled and presented in the next section.

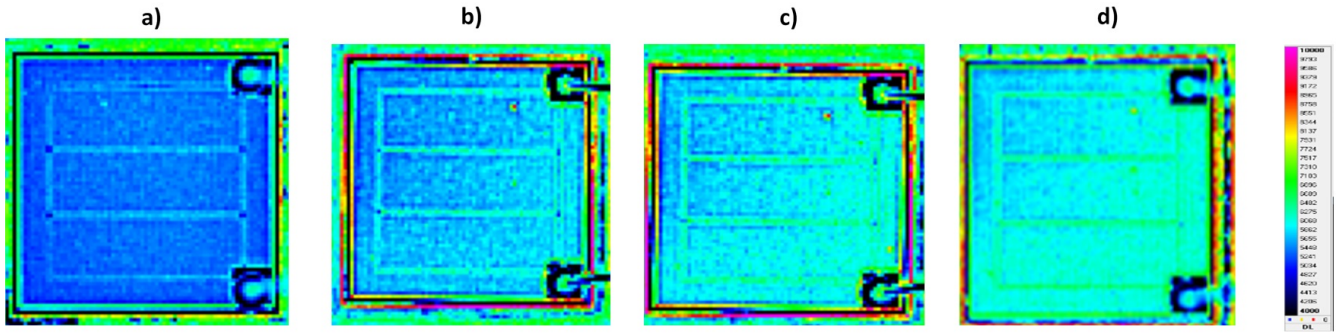


Figure 6: Thermal analysis of a LED with forward current at 350mA: a) before the test; b) at 576h; c) at 720h and d) at 1500h

Table 3: Increment of junction temperature due to the LEDs' degradation under stress of $T = 85^{\circ}C$

Component	$\Delta T(t) [^{\circ}C]$			
	$t = 0h$	$t = 576h$	$t = 720h$	$t = 1500h$
1	0	2.4	3.4	5.7
2	0	2.5	3.6	7.0
3	0	2.7	3.8	7.2
4	0	1.6	2.6	5.5
5	0	2.0	3.0	6.2
6	0	2.4	3.4	6.0
7	0	2.5	3.3	5.7
8	0	2.2	3.9	7.0
9	0	2.3	3.7	5.3
Average	0	2.28	3.41	5.5

Table 4: Increment of junction temperature due to the LEDs' degradation under stress of $T = 100^{\circ}C$

Component	$\Delta T(t)$ [$^{\circ}C$]			
	$t = 0h$	$t = 576h$	$t = 720h$	$t = 1500h$
1	0	2.6	3.8	6.7
2	0	3.8	5.3	9.5
3	0	3.7	4.7	9.0
4	0	3.5	4.5	9.2
5	0	3.0	4.3	7.8
6	0	4.2	5.2	9.2
7	0	2.9	4.0	8.3
8	0	2.5	3.1	5.8
9	0	3.7	4.7	8.7
10	0	4.8	6.0	10.5
Average	0	3.47	4.56	8.47

3 Mathematical modelling of self-heating impact

In this section, we try to model the impact of self-heating phenomenon in the LED's accelerated degradation process.

As the normalized **luminous intensity** is decreasing overtime under a given stress temperature, the degradation indicator of the LED is built as follows

$$X(t) = 1 - P_{out}(t) \quad (3)$$

In that way, $X(t)$ is an increasing process, see Figure 7.

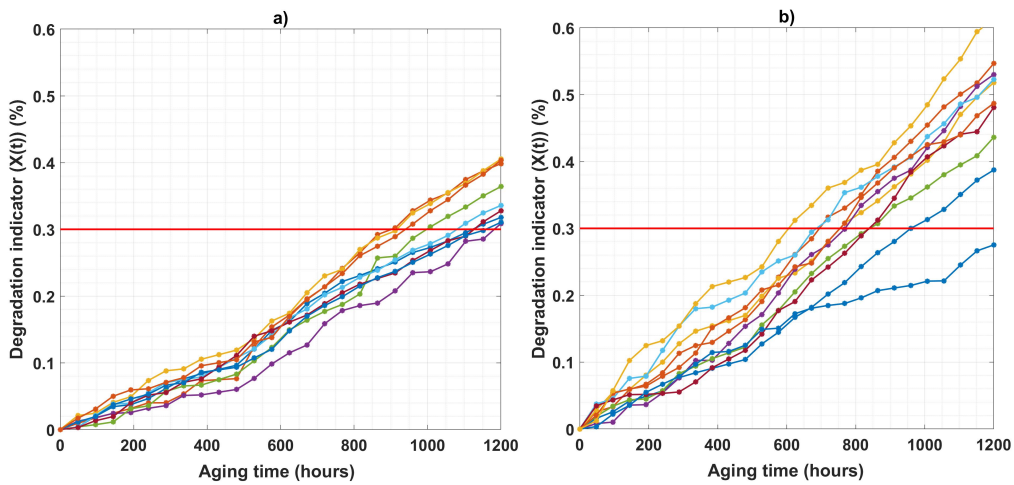


Figure 7: Degradation indicator at two stress conditions ; a) $T_1 = 85^{\circ}C$; b) $T_2 = 100^{\circ}C$

3.1 Conventional degradation rate model

According to the Arrhenius reaction rate theory [11], the degradation rate $\mu(T_k)$ under stress temperature T_k can be formulated by:

$$\mu(T_k) = \alpha \times \exp\left(-\frac{\beta}{T_j}\right) \quad (4)$$

Where

- T_j is the junction temperature and it is considered as the stress temperature, i.e., $T_j = T_k$.
- α and β represent the characteristics of the LED failure mechanism and test conditions. β can be expressed as

$$\beta = \frac{E_a}{k_B},$$

with E_a is the activation energy for the reaction and k_B is the Boltzmann constant.

According to this model, the degradation rate depends only on the failure mechanism and the magnitude of the junction temperature T_j , which is considered the constant stress temperature. This means that the degradation rate is constant.

3.2 Modified degradation rate model with self-heating impact

As shown in section 4.3, the LED's junction temperature might increase during the acceleration tests due to the appearance of defects [16, 12]. In fact, as mentioned above, the increment in the junction temperature can be divided into two parts:

- Power dissipation effect: when a forward current is applied to a LED, the LED's junction generates heat, which in turn increases the temperature of the LED's junction. This heat depends not only on the forward current but also on the LED's design (related to thermal resistance), see Figure 5.
- The impact of degradation: this means that when the degradation occurs, it increases the LED junction temperature, see Figure 6.

However, this variation in junction temperature is not considered in the conventional degradation rate model. We propose herein a modified degradation rate allowing considering the self-heating impact, i.e., the increasing of the junction temperature. In this way, the increasing of the junction temperature, with respect to the stress temperature, can be expressed as follows:

$$\Delta\mathcal{T}(t) = a + f(X(t)) \quad (5)$$

where,

- a is a non-negative real number and depends on the forward current and the characteristics of structure and material of the LED, see Appendix A. In this study, we assume that a is constant if the forward current is constant; it can be estimated in the analysis step.
- $f(X(t))$ indicates the effect of the degradation state, $X(t)$, on the LED degradation process.

Moreover, we suppose that the effect of the degradation state, $f(X(t))$, can be described as Eq. (6) for a simplified model. A detailed explanation is shown in Appendix A.

$$f(X(t)) = b.X(t) \quad (6)$$

where b is a non-negative real number that qualifies the influence of the LED's degradation state on its accelerated degradation rate. According to Eq. (5) and Eq. (6), the junction temperature can be calculated by $\mathcal{T}_j = T_k + \Delta\mathcal{T} = T_k + a + b.X(t)$. So, the formulation of the LED's degradation rate can be extended by considering the self-heating as follows:

$$\mu(T_k, t) = \alpha \times \exp\left(-\frac{\beta}{T_k + a + b.X(t)}\right) \quad (7)$$

This model somehow shows the state-dependence effect, i.e., the degradation evolution depends on the current degradation level [20, 21].

4 Degradation modelling and reliability assessment

From the degradation rate, the evolution of the degradation process considering the self-heating impact can be derived using modified stochastic difference equation (SDE) [22, 20].

$$dX(t) = \mu(T_k, t).dt + \sigma.dB(t) \quad (8)$$

where $B(t)$ is a standard Brownian motion with the following properties:

- $B(0) = 0$, where $B(t) \in [0, \infty)$,
- Station and independent increments, namely $B(t + \Delta t) - B(t) \sim N(0, \Delta t)$; where σ is the diffusion parameter, σ is a constant and $\sigma > 0$.

4.1 Degradation model

Following the accelerated degradation rate model considering the self-heating, we formulate a degradation model of a LED and its reliability calculation. Note however that determining the analytically formulation of $X(t)$ based on Eq. (8) and Eq. (7) is very challenging [22]. Thus, we propose to use an approximation by the Taylor series, and the degradation rate of the component can be expressed by :

$$\mu(T_k', t) = \alpha \cdot \left[e^{\left(-\frac{\beta}{T_k'}\right)} + b \times \frac{\beta}{T_k'^2} \cdot e^{\left(-\frac{\beta}{T_k'}\right)} \times X(t) \right] \quad (9)$$

where, $T'_k = T_k + a$.

By using Eq. (9), Eq. (8) can be written as follows:

$$dX(t) = \lambda. [\kappa + X(t)] dt + \sigma.dB(t) \quad (10)$$

where:

$$\kappa = \frac{T_k'^2}{b\beta} \quad (11)$$

$$\lambda = b \times \frac{\alpha\beta}{T_k'^2} \cdot \exp\left(-\frac{\beta}{T_k'}\right) \quad (12)$$

Finally, the LED' degradation model considering the self-heating is found as the explicit solution of Eq.(10), [20]:

$$X(t) = X(0).e^{\lambda.t} + \kappa \left(e^{\lambda.t} - 1\right) + \int_0^t \sigma.e^{\lambda(t-s)} dB(s).ds \quad (13)$$

A detailed mathematical development of Equation (10) is shown in Appendix B.

4.2 Reliability assessment

With a failure threshold, denoted D , the failure time is defined as the first hitting time of the stochastic degradation process exceeding the failure threshold value D . Then the cumulative failure distribution function can be expressed as:

$$\begin{aligned} F(t) &= P(X(t) > D) \\ &= \Phi\left(\frac{E(X(t)) - D}{\sqrt{Var(X(t))}}\right) \end{aligned} \quad (14)$$

where $E(X(t))$, $Var(X(t))$ are the mathematical expectation and the variance of $X(t)$ respectively.

$$\begin{aligned} E(X(t)) &= E\left(X(0).e^{\lambda.t} + \kappa \left(e^{\lambda.t} - 1\right)\right) \\ &+ E\left(\int_0^t \sigma.e^{\lambda(t-s)} dB(s).ds\right) \end{aligned} \quad (15)$$

Note that $E(X(0).e^{\lambda.t} + \kappa(e^{\lambda.t} - 1))$ are deterministic values for any given t , whereas $E\left(\int_0^t \sigma.e^{\lambda(t-s)} dB(s).ds\right) = 0$. Thus,

$$E(X(t)) = X(0).e^{\lambda.t} + \kappa \left(e^{\lambda.t} - 1\right) \quad (16)$$

The variance of $X(t)$ can be expressed as:

$$\begin{aligned} Var(X(t)) &= Var\left(\int_0^t \sigma \cdot \exp(\lambda(t-s)) dB(s).ds\right) \\ &= \sigma^2 \times \int_0^t \exp(2.\lambda(t-s)) .ds \\ &= \frac{\sigma^2}{2.\lambda} (\exp(2.\lambda.t) - 1) \end{aligned} \quad (17)$$

Finally, from Eq. (14) the reliability of the LED can be evaluated by:

$$\begin{aligned} R(t) &= 1 - F(t) \\ &= 1 - \Phi\left(\frac{E(X(t)) - D}{\sqrt{Var(X(t))}}\right) \end{aligned} \quad (18)$$

4.3 Parameters estimation

The proposed model is characterized by a set of parameters $\theta = \{\alpha, \beta, a, b, \sigma\}$ which need to be estimated from the experimental data. Noting that a can be directly estimated with the analytical step [23] thanks to an infrared camera. To estimate the remaining parameters $(\alpha, \beta, b, \sigma)$ from the experimental data, we develop herein an estimation approach based on the discrete maximum likelihood (DML) [24, 20]. Indeed, the degradation level at time t can be expressed by:

$$X(t_j) = X(t_{j-1}) + \kappa \left(e^{\lambda \cdot \Delta t} - 1 \right) + e^{\lambda \cdot \Delta t} \cdot X(t_{j-1}) + \sigma^* \cdot dB(t_j) \quad (19)$$

where,

$$(\sigma^*)^2 = \frac{\sigma^2}{2 \cdot \lambda} \left(e^{2 \cdot \lambda \cdot \Delta t} - 1 \right) \quad (20)$$

Suppose that degradation signals are monitored at separated times, and $\Delta t = t_j - t_{(j-1)}$ is the measurement frequency and Δt is small enough. According to Ito's stochastic integral [25], the conditional probability density of an observation $X(t_j)$ given the previous observation $X(t_{j-1})$, with Δt being time step, is given by

$$f(X(t_j)|X(t_{j-1}), \kappa, \lambda, \sigma^*) = \frac{1}{\sqrt{2\pi (\sigma^*)^2}} \cdot \exp \left(- \frac{[X(t_j) - \kappa (e^{\lambda \cdot \Delta t} - 1) - e^{\lambda \cdot \Delta t} \cdot X(t_{j-1})]^2}{2 (\sigma^*)^2} \right) \quad (21)$$

Then, the log-likelihood function of an observation data can be as follows:

$$l(\alpha, \beta, b, \sigma) = \sum_{k=1}^K \sum_{i=1}^{n_k} \sum_{j=1}^{m_k} \ln (f(X(t_j)|X(t_{j-1}), \alpha, \beta, b, \sigma)) \quad (22)$$

The partial derivations for maximum likelihood estimation are required and set equal to zero, i.e.,

$$\begin{aligned} \frac{\partial l(\alpha, \beta, b, \sigma)}{\partial \alpha} &= 0 \\ \frac{\partial l(\alpha, \beta, b, \sigma)}{\partial \beta} &= 0 \\ \frac{\partial l(\alpha, \beta, b, \sigma)}{\partial b} &= 0 \\ \frac{\partial l(\alpha, \beta, b, \sigma)}{\partial \sigma} &= 0 \end{aligned} \quad (23)$$

By using a numerical method for nonlinear algebraic equations, the parameters $(\alpha, \beta, b, \sigma)$ can be obtained by integrally solving the partial derivative equations using a MATLAB procedure of the Nelder-Mead simplex method [26]. A detailed mathematical development of (23) is shown in Appendix C.

5 Result analyses

In this section, we analyse some obtained results when applying the proposed degradation model to our experimental dataset.

5.1 Estimation of degradation parameters and reliability

First, a can be easily estimated by the fact that the forward current at 350ma leads to an increasing of 10 degrees in the junction temperature (see again section 2), i.e., $\hat{a} = 10$. The other parameters α, β, b, σ are estimated by the estimation approach presented in section 4.3. The obtained results are reported in Table 5. Especially, the decay rate following the convention ADT under two stresses of temperature $85^\circ C$ and $100^\circ C$ is found at $3.5E - 4, 5.7E - 4$, respectively. Note that the conventional ADT and the estimation method are presented in Appendix D.

Table 5: Parameters estimation

Terms	Parameter	
	Mean	std
$\hat{\alpha}$	4.5	0.1
$\hat{\beta}(\times 10^3)$	3.6	0.2
\hat{a}	10	2
\hat{b}	16.78	2.72
$\hat{\sigma}$	0.002	-

Next, an additional analysis on LED shows some small darkening in the junction mesa; see Figure 8. These defects are directly related to LEDs degradation and failure. Besides, we did not observe any defects in the electrode metal contact region after the acceleration test. This failure mechanism of bulk defects coincides with the energy activation, about $E_a = 0.31eV$, which is found based on the model parameter's estimated value. Therefore, it can be concluded that the performance of the estimates seems to be adequate.

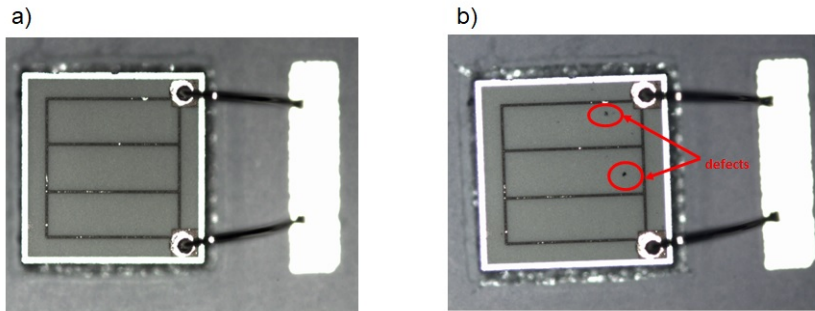


Figure 8: A result of the optical microscopy analysis: a) before the test; b) after the test

Moreover, the **luminous intensity** of LEDs, see Figure 4, has degraded to 70% of their initial value. Thus, the t_{L70} of each LED under two stress levels ($T_1 = 85^\circ C, T_2 = 100^\circ C$) are given in Table 6 and Table 7 respectively.

Table 6: Result of acceleration test under stress $T_1 = 85^\circ C$

Component	t_{L70} [h]	Uncertainty [h]
1	867	$[-38, +10]$
2	916	$[-14, +34]$
3	939	$[-28, +20]$
4	997	$[-37, +11]$
5	1030	$[-24, +24]$
6 and 7	1135	$[-22, +26]$
8	1218	$[-30, +18]$
9	1569	$[-17, +31]$

Table 7: Result of acceleration test under stress $T_2 = 100^\circ C$

Component	t_{L70} [h])	Uncertainty [h]
1	605	$[-30, +18]$
2 and 3	681	$[-20, +28]$
4	712	$[-23, +25]$
5	754	$[-25, +23]$
6	769	$[-18, +30]$
7	840	$[-25, +23]$
8	912	$[-37, +11]$
9 and 10	1230	$[-18, +30]$

5.2 Comparison analysis

According to Eq. (14), the cumulative distribution function (CDF) based on the proposed degradation model is calculated using the estimated parameters reported in table 5. The obtained results are then compared with the experiment dataset in tables 6 and 7, see figures 9 and 10. It is clearly found that the CDF based on the proposed degradation model, which considers self-heating, is well-fitting with the experiment values. In contrast, without self-heating consideration, the conventional ADT model (see Appendix D) leads to a significant error in the calculation of CDF.

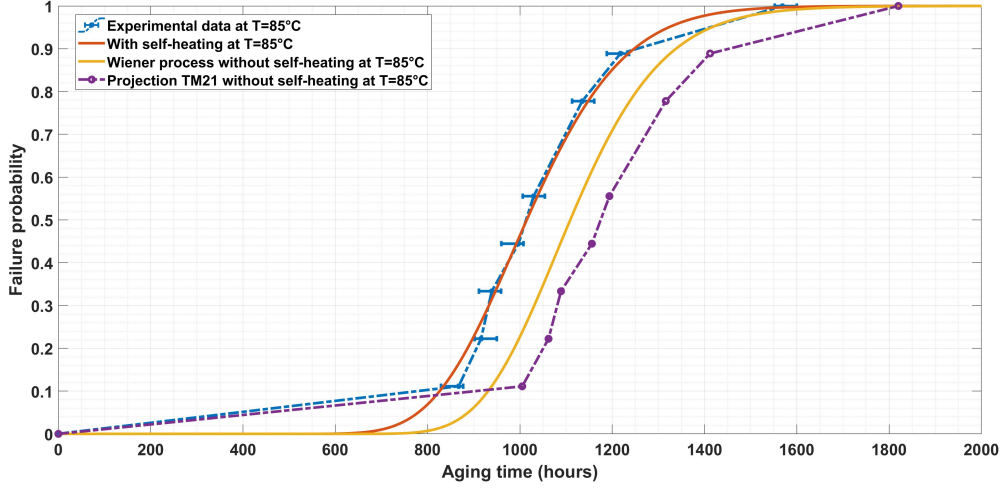


Figure 9: Cumulative failure function of LED according to Eq. 14 and the value experimental under stress at $85^{\circ}C$

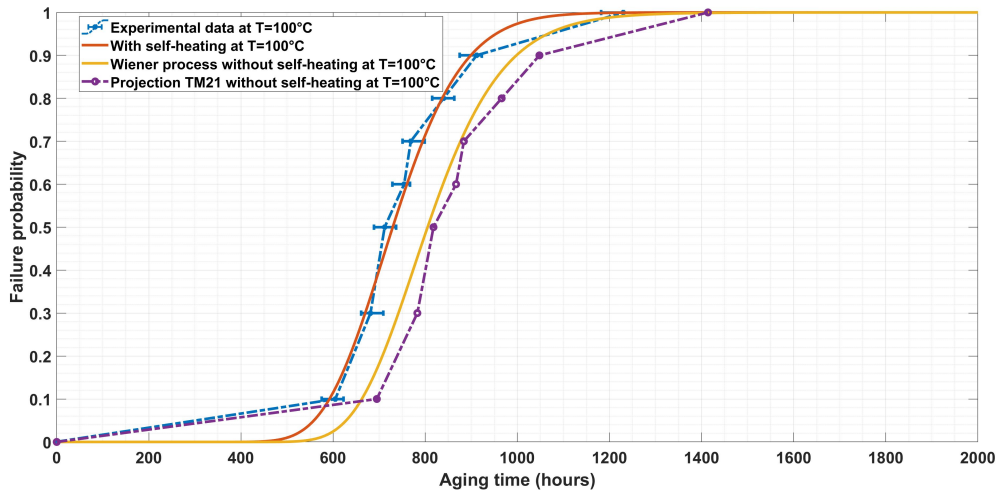


Figure 10: Cumulative failure function of LED according to Eq. (14) and the value experimental under stress at $100^{\circ}C$

Figure 11 and Figure 12 show the LED's reliability with and without self-heating consideration under the stress temperature at $T_1 = 85^{\circ}C$ and $T_2 = 100^{\circ}C$. The obtained results show that without

considering the self-heating impact in the degradation process of a LED leads to a significant error in the LED reliability assessment.

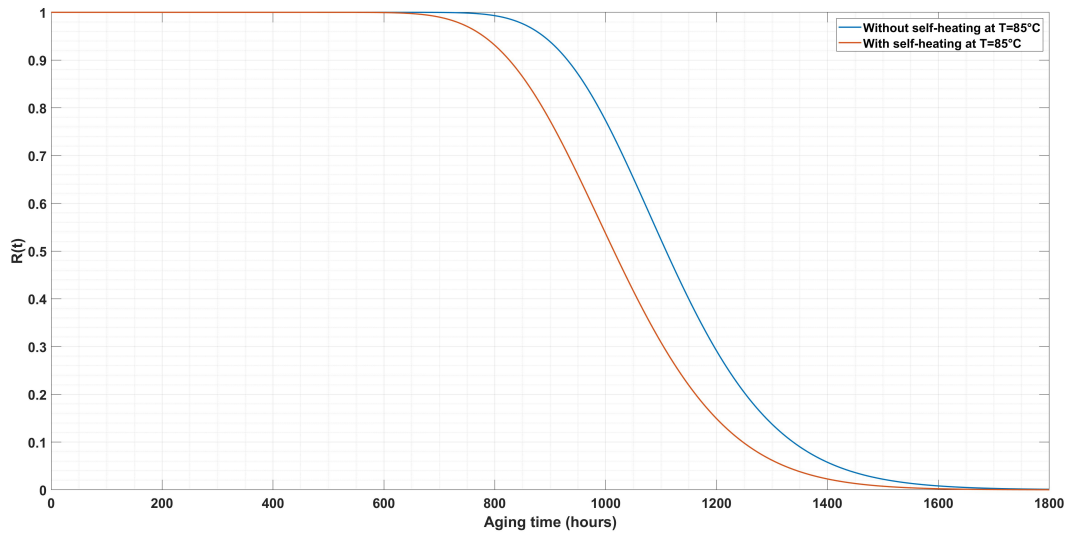


Figure 11: Reliability of LED under stress at $85^{\circ}C$

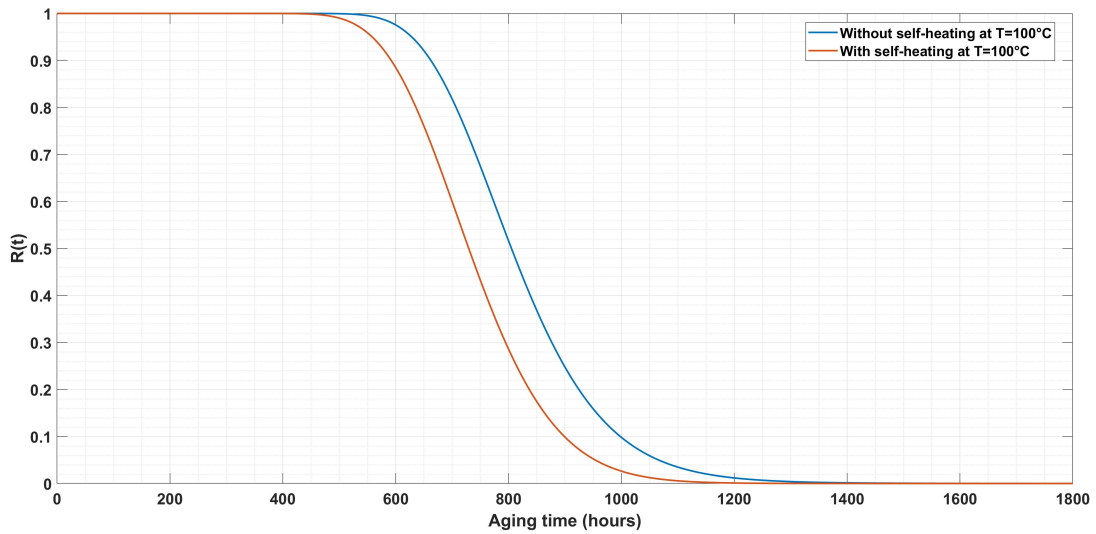


Figure 12: Reliability of LED under stress at $100^{\circ}C$

5.3 Evolution of the junction temperature

As an illustration, figure 13 shows simulated paths of the junction temperature over time using the proposed model with estimated parameters which are reported table 5.

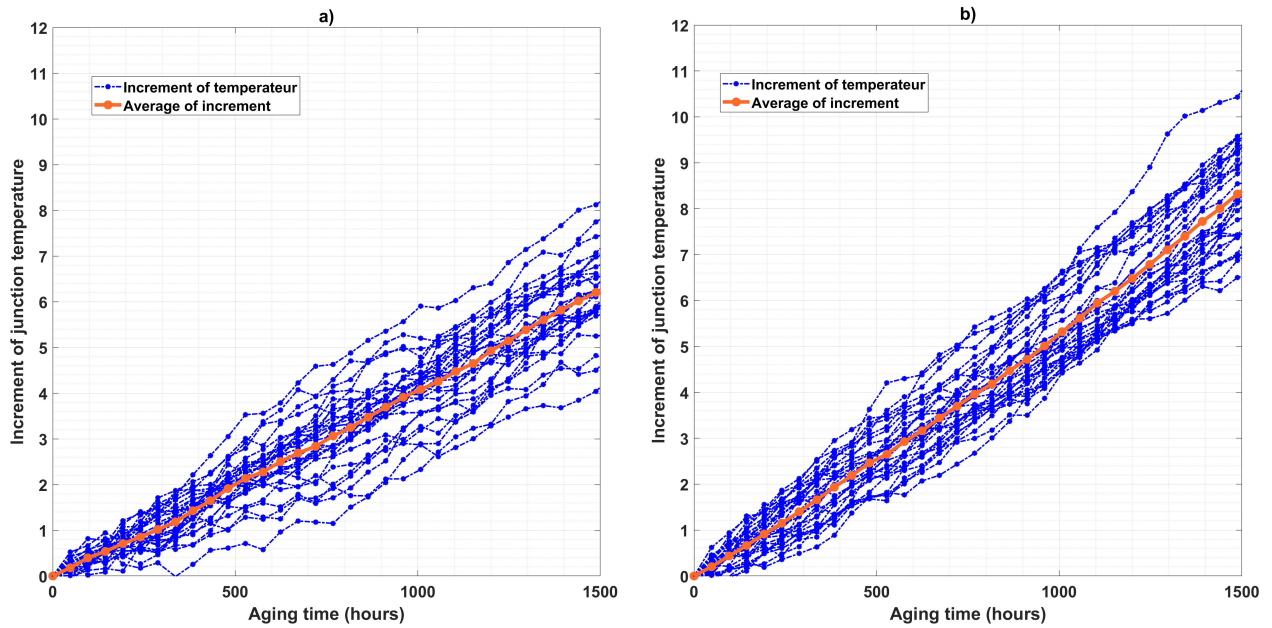


Figure 13: Simulated paths of the junction temperature with a) $T_1 = 85^\circ C$ and b) $T_2 = 100^\circ C$

Table 8 reports the average simulated increments on the the junction temperature at several time points t ($t = 0, 576, 720, 1500h$).

Table 8: Increment of the junction temperature obtained from the simulated paths

	$\Delta T(t)$ [$^\circ C$]			
Stress	$t = 0$	$t = 576h$	$t = 720h$	$t = 1500h$
$85^\circ C$	0	2.28	3.29	6.23
$100^\circ C$	0	3.43	4.53	8.37

It is clear that the simulated results are very closed to the experimental ones (see tables 3 and 4).

5.4 Sensitivity analysis to data samples:

In this section, we examine the impact of the data samples on the reliability assessment or CDF of the LED. In that way, two data samples are used. The first is the data samples from 0 to 576h, and the second is from 0 to 720h. Figures 14 and 15 present the CDF of the proposed degradation model with two different data samples. The results show that the CDF built with the samples of 720h is well-fitting with the experiment values. It is also very closed to the results obtained with the full dataset ($t = 1500h$). Besides, a significant error is obtained when using the samples of 576h. This can be explained that 576h data samples are not sufficient to provide good estimators while an accelerated dataset until $t = 720h$ is quite enough to get a good estimator that allows obtaining a good accuracy for the LED's reliability assessment. This is an interesting result that allows us to stop the accelerated test from $t = 720h$ while ensuring the accuracy of the reliability assessment of the LED component.

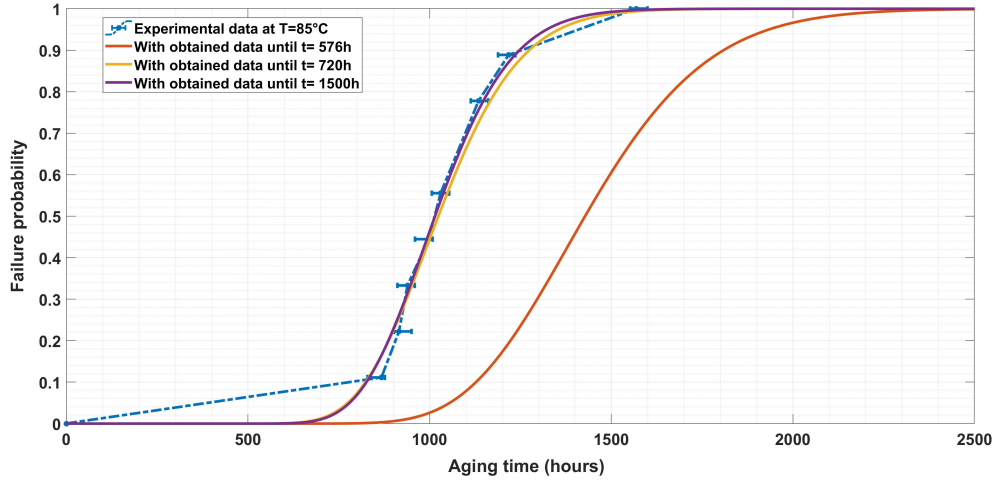


Figure 14: Cumulative failure function estimated with different data samples under stress at $85^{\circ}C$

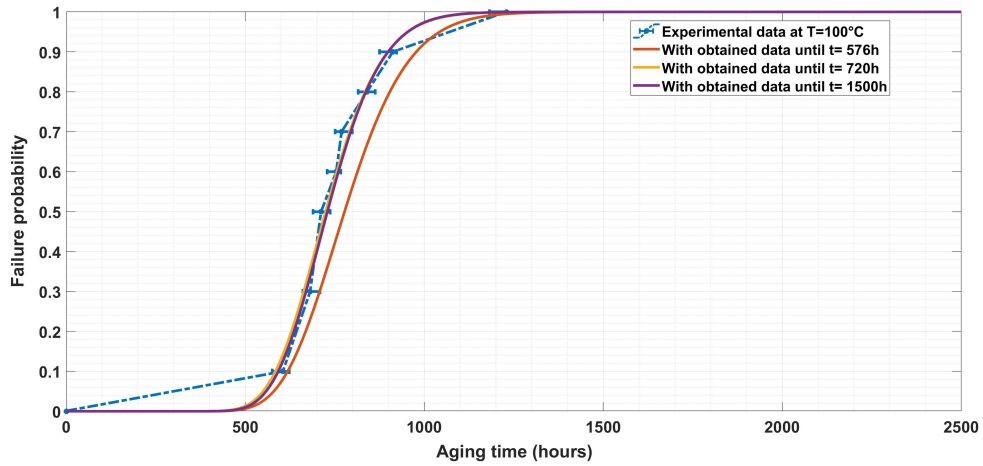


Figure 15: Cumulative failure function estimated with different data samples under stress at $100^{\circ}C$

6 Conclusions

This paper proposes a novel accelerated degradation model for a LED component considering self-heating phenomenon, i.e., increasing of the junction temperature due to both the environmental stress and the degradation behavior of the LED component. The proposed degradation model allows assessing more precisely the reliability of LED components under a stress condition. In that way, the self-heating impact is firstly analysed from experimental data and then mathematically formulated. To consider the self-heating impact on the LED's degradation process, a [modified](#) accelerated degradation model is developed based on a modified stochastic difference equation. Then the reliability of LED component is formulated. To estimate the proposed model's parameters, an estimation approach is also proposed. Finally, the proposed degradation model is applied for a real dataset of 19 identical LED components. The obtained results show that the proposed degradation model fits well

to the experimental data. Also, it is shown that without considering the self-heating may lead to a significant error in the reliability assessment of LED components. Our future research works will focus on the development of the proposed model for a more complex system with self-heating and thermal interactions between components.

Appendix

Appendix A. Increasing of the junction temperature caused by the self-heating impact

As a semiconductor device which emits the light, the electrical power consumed by the LED principally converts into light and heat dissipation.

$$P_{electrical} = P_{light} + P_{heat} \quad (24)$$

Then, [27, 28] show the relation between LED junction temperature and the [luminous intensity](#), forward voltage following Eq.(25).

$$\begin{aligned} T_j &= T_k + R_{th} \cdot (I \cdot V_f - P) \\ V_f &= A + B \cdot T_j \end{aligned} \quad (25)$$

where, T_k is the ambient temperature, R_{th} is the thermal resistance, $I \cdot V_f$ is the input electrical power, and P is [luminous intensity](#); A and B represent the constant coefficient.

- When $t = 0$, due to heat dissipation, the junction temperature increases about a .
- Then, the relation between the [luminous intensity](#) and the junction temperature over time according to the following equation:

$$\begin{aligned} P_{out}(t) &= \frac{P(t)}{P(0)} = c + d \cdot T_j(t) \\ X(t) &= 1 - P_{out}(t) = \frac{d \cdot \Delta T_j(t)}{c + d \cdot T_j(0)} \\ \Delta T_j(t) &= \frac{c + d \cdot T_j(0)}{d} \cdot X(t) = b \cdot X(t) \end{aligned} \quad (26)$$

Thus, the increasing of the junction temperature affecting the LED degradation can be modeled as Eq. (6)

Appendix B. Resolution of Equation (10)

We try to find the explicit solution of (10). In order to solve the SDE equation, we introduce then some transformations as follows.

- The expression $exp(-\lambda \cdot s)$ satisfies the following equation

$$dexp(-\lambda \cdot s) = -\lambda \times exp(-\lambda \cdot s) ds \quad (27)$$

- Next, we consider the difference of $\exp(-\lambda.s) \times X(s)$. By using Ito's formula, we have

$$d(\exp(-\lambda.s) \times X(s)) = -\lambda.\exp(-\lambda.s).X(s).ds + \exp(-\lambda.s) \times dX(s) + 0 \quad (28)$$

- Then, we have

$$\begin{aligned} d(\exp(-\lambda.s) \times X(s)) &= -\lambda.\exp(-\lambda.s).X(s).ds \\ &\quad + \exp(-\lambda.s) [\lambda. [\kappa + X(s)] ds + \sigma.dB(s)] \\ &= \exp(-\lambda.s).\lambda.\kappa.ds + \sigma.\exp(-\lambda.s).dB(s) \end{aligned} \quad (29)$$

- Integrating both side from 0 to t, we have:

$$\exp(-\lambda.t) \times X(t) - X(0) = \int_0^t \exp(-\lambda.s).\lambda.\kappa.ds + \int_0^t \sigma.\exp(-\lambda.s).dB(s) \quad (30)$$

- So

$$X(t) = \exp(\lambda.t).X(0) + \int_0^t \exp[\lambda.(t-s)].\lambda.\kappa.ds + \int_0^t \sigma.\exp[\lambda.(t-s)].dB(s) \quad (31)$$

Appendix C. First deviated of log-likelihood function

$$\begin{aligned}
 \frac{\partial l(\alpha, \beta, b, \sigma)}{\partial \alpha} = & \frac{2\alpha\beta^2 e^{-\frac{\beta}{T_k} fb^2} e^{-\frac{2\alpha\beta e^{-\frac{\beta}{T_k} fb}}{T_k'^2} - \frac{\beta}{T_k}} \left(X(t_j) - e^{-\frac{\beta}{T_k} fb} X(t_{j-1}) - \frac{T_k'^2 \left(e^{\frac{\alpha\beta e^{-\frac{\beta}{T_k} fb}}{T_k'^2} - 1} \right)}{\beta b} \right)^2}{T_k'^4 \sigma^2 \left(e^{\frac{2\alpha\beta e^{-\frac{\beta}{T_k} fb}}{T_k'^2} - 1} \right)^2} \\
 & - \frac{\beta e^{-\frac{\beta}{T_k} b} \left(X(t_j) - e^{-\frac{\beta}{T_k} fb} X(t_{j-1}) - \frac{T_k'^2 \left(e^{\frac{\alpha\beta e^{-\frac{\beta}{T_k} fb}}{T_k'^2} - 1} \right)}{\beta b} \right)^2}{\alpha\beta e^{-\frac{\beta}{S} b} \left(\frac{2e^{\frac{\beta}{S} \sigma^2} f e^{-\frac{2\alpha\beta e^{-\frac{\beta}{S} fb}}{S^2} - \frac{\beta}{S}} \pi - S^2 e^{\frac{\beta}{S} \sigma^2} \left(e^{\frac{2\alpha\beta e^{-\frac{\beta}{S} fb}}{S^2} - 1} \right) \pi}{\alpha^2 \beta b} \right)} \\
 & - \frac{T_k'^2 \sigma^2 \left(e^{\frac{2\alpha\beta e^{-\frac{\beta}{T_k} fb}}{T_k'^2} - 1} \right)}{2S^2 \sigma^2 \left(e^{\frac{2\alpha\beta e^{-\frac{\beta}{S} fb}}{S^2} - 1} \right) \pi} \\
 & - \frac{2\alpha\beta e^{-\frac{\beta}{T_k} b} \left(-\frac{\beta f b e^{-\frac{\beta}{T_k} fb}}{T_k'^2} - \frac{\beta}{T_k} X(t_{j-1}) - f e^{-\frac{\beta}{T_k} fb} - \frac{\beta}{T_k} \right) \left(X(t_j) - e^{-\frac{\beta}{T_k} fb} X(t_{j-1}) - \frac{T_k'^2 \left(e^{\frac{\alpha\beta e^{-\frac{\beta}{T_k} fb}}{T_k'^2} - 1} \right)}{\beta b} \right)}{T_k'^2 \sigma^2 \left(e^{\frac{2\alpha\beta e^{-\frac{\beta}{T_k} fb}}{T_k'^2} - 1} \right)}
 \end{aligned}$$

(32)

$$\begin{aligned}
& \alpha\beta e^{-\frac{\beta}{T_k'} b} \left(\frac{-\frac{\beta}{T_k'}}{2\alpha e^{\frac{-\beta}{T_k'} fb} - \frac{-\beta}{T_k'}} \right) e^{\frac{2\alpha\beta e^{-\frac{\beta}{T_k'} fb}}{T_k'}} X(t_j) - e^{\frac{-\beta}{T_k'} fb} X(t_{j-1}) - \frac{T_k'^2 \left(e^{\frac{\alpha\beta e^{-\frac{\beta}{T_k'} fb}}{T_k'}} - 1 \right)}{\beta b} \Bigg)^2 \\
\frac{\partial l(\alpha, \beta, b, \sigma)}{\partial \beta} = & \frac{\left(T_k'^2 \sigma^2 \left(e^{\frac{2\alpha\beta e^{-\frac{\beta}{T_k'} fb}}{T_k'}} - 1 \right) \right)^2}{\left(\alpha\beta e^{-\frac{\beta}{T_k'} b} \left(X(t_j) - e^{\frac{-\beta}{T_k'} fb} X(t_{j-1}) - \frac{T_k'^2 \left(e^{\frac{\alpha\beta e^{-\frac{\beta}{T_k'} fb}}{T_k'}} - 1 \right)}{\beta b} \right) \right)^2} \\
& + \frac{\left(\alpha e^{-\frac{\beta}{T_k'} b} \left(X(t_j) - e^{\frac{-\beta}{T_k'} fb} X(t_{j-1}) - \frac{T_k'^2 \left(e^{\frac{\alpha\beta e^{-\frac{\beta}{T_k'} fb}}{T_k'}} - 1 \right)}{\beta b} \right) \right)^2}{\left(T_k'^3 \sigma^2 \left(e^{\frac{2\alpha\beta e^{-\frac{\beta}{T_k'} fb}}{T_k'}} - 1 \right) \right)} - \frac{\left(T_k'^2 \sigma^2 \left(e^{\frac{2\alpha\beta e^{-\frac{\beta}{T_k'} fb}}{T_k'}} - 1 \right) \right)}{\left(2\alpha\beta e^{-\frac{\beta}{T_k'} b} \left(- \left(\frac{-\frac{\beta}{T_k'}}{\alpha e^{\frac{-\beta}{T_k'} fb} - \frac{-\beta}{T_k'}} \right) e^{\frac{\alpha\beta e^{-\frac{\beta}{T_k'} fb}}{T_k'}} X(t_{j-1}) - \frac{T_k'^2 \left(\frac{-\frac{\beta}{T_k'}}{\alpha e^{\frac{-\beta}{T_k'} fb} - \frac{-\beta}{T_k'}} - \alpha\beta e^{\frac{-\beta}{T_k'} fb} \right) e^{\frac{-\beta}{T_k'} fb} X(t_{j-1}) - \frac{T_k'^2 \left(\frac{-\beta}{\alpha e^{\frac{-\beta}{T_k'} fb} - \frac{-\beta}{T_k'}} - \alpha\beta e^{\frac{-\beta}{T_k'} fb} \right) e^{\frac{-\beta}{T_k'} fb} X(t_{j-1}) - \frac{T_k'^2 \left(e^{\frac{\alpha\beta e^{-\frac{\beta}{T_k'} fb}}{T_k'}} - 1 \right)}{\beta b} + \frac{T_k'^2 \left(e^{\frac{\alpha\beta e^{-\frac{\beta}{T_k'} fb}}{T_k'}} - 1 \right)}{\beta^2 b} \right) \right)} \\
& - \frac{\left(T_k'^2 \sigma^2 \left(e^{\frac{2\alpha\beta e^{-\frac{\beta}{T_k'} fb}}{T_k'}} - 1 \right) \right)}{\left(\alpha\beta e^{-\frac{\beta}{T_k'} b} \left(X(t_j) - e^{\frac{-\beta}{T_k'} fb} X(t_{j-1}) - \frac{T_k'^2 \left(e^{\frac{\alpha\beta e^{-\frac{\beta}{T_k'} fb}}{T_k'}} - 1 \right)}{\beta b} \right) \right)} \\
& - \frac{\left(T_k'^2 \sigma^2 \left(e^{\frac{2\alpha\beta e^{-\frac{\beta}{T_k'} fb}}{T_k'}} - 1 \right) \right)}{\left(\alpha\beta e^{-\frac{\beta}{T_k'} b} \left(\frac{T_k'^2 \sigma^2 \left(\frac{-\frac{\beta}{T_k'}}{2\alpha e^{\frac{-\beta}{T_k'} fb} - \frac{-\beta}{T_k'}} - \frac{-\beta}{T_k'} \right) e^{\frac{2\alpha\beta e^{-\frac{\beta}{T_k'} fb}}{T_k'}} + \frac{\beta}{T_k'} \pi \right) + \frac{T_k' e^{\frac{\beta}{T_k'} \sigma^2} \left(e^{\frac{2\alpha\beta e^{-\frac{\beta}{T_k'} fb}}{T_k'}} - 1 \right) \pi}{\alpha\beta b} - \frac{T_k'^2 e^{\frac{\beta}{T_k'} \sigma^2} \left(e^{\frac{2\alpha\beta e^{-\frac{\beta}{T_k'} fb}}{T_k'}} - 1 \right) \pi}{\alpha\beta^2 b} \right)} \\
& - \frac{\left(2T_k'^2 \sigma^2 \left(e^{\frac{2\alpha\beta e^{-\frac{\beta}{T_k'} fb}}{T_k'}} - 1 \right) \pi \right)}{\left(\alpha\beta e^{-\frac{\beta}{T_k'} b} \left(X(t_j) - e^{\frac{-\beta}{T_k'} fb} X(t_{j-1}) - \frac{T_k'^2 \left(e^{\frac{\alpha\beta e^{-\frac{\beta}{T_k'} fb}}{T_k'}} - 1 \right)}{\beta b} \right) \right)}
\end{aligned}$$

(33)

$$\begin{aligned}
\frac{\partial l(\alpha, \beta, b, \sigma)}{\partial b} = & \frac{2\alpha^2 \beta^2 e^{-\frac{\beta}{T_k'} f b e} \frac{2\alpha\beta e^{-\frac{\beta}{T_k'} f b} - \frac{\beta}{T_k'}}{T_k'^2} - \frac{\beta}{T_k'} \left(X(t_j) - e^{-\frac{\beta}{T_k'} f b} X(t_{j-1}) - \frac{e^{-\frac{\beta}{T_k'} f b} \left(\frac{\alpha\beta e^{-\frac{\beta}{T_k'} f b}}{T_k'^2} - 1 \right)}{\beta b} \right)^2}{T_k'^4 \sigma^2 \left(e^{-\frac{\beta}{T_k'} f b} \frac{2\alpha\beta e^{-\frac{\beta}{T_k'} f b}}{T_k'^2} - 1 \right)^2} \\
& - \frac{\alpha\beta e^{-\frac{\beta}{T_k'} f b} \left(X(t_j) - e^{-\frac{\beta}{T_k'} f b} X(t_{j-1}) - \frac{e^{-\frac{\beta}{T_k'} f b} \left(\frac{\alpha\beta e^{-\frac{\beta}{T_k'} f b}}{T_k'^2} - 1 \right)}{\beta b} \right)^2}{\alpha\beta e^{-\frac{\beta}{T_k'} f b} b} \left(\frac{2\alpha\beta e^{-\frac{\beta}{T_k'} f b} - \frac{\beta}{T_k'}}{2e^{-\frac{\beta}{T_k'} f b} \sigma^2} - \frac{\beta}{T_k'} \pi \right) \frac{\left(\frac{2\alpha\beta e^{-\frac{\beta}{T_k'} f b}}{T_k'^2} - 1 \right) \pi}{\alpha\beta h^2} \\
& - \frac{T_k'^2 \sigma^2 \left(e^{-\frac{\beta}{T_k'} f b} \frac{2\alpha\beta e^{-\frac{\beta}{T_k'} f b}}{S^2} - 1 \right)}{2T_k'^2 \sigma^2 \left(e^{-\frac{\beta}{T_k'} f b} \frac{2\alpha\beta e^{-\frac{\beta}{T_k'} f b}}{T_k'^2} - 1 \right) \pi} \\
& - \frac{2\alpha\beta e^{-\frac{\beta}{T_k'} f b} \left(-\frac{\alpha\beta f e^{-\frac{\beta}{T_k'} f b} - \frac{\beta}{T_k'} x}{T_k'^2} - \frac{\alpha\beta e^{-\frac{\beta}{T_k'} f b} - \frac{\beta}{T_k'}}{b} + \frac{T_k'^2 \left(\frac{\alpha\beta e^{-\frac{\beta}{T_k'} f b}}{T_k'^2} - 1 \right)}{\beta T_k'^2} \right) \left(X(t_j) - e^{-\frac{\beta}{T_k'} f b} X(t_{j-1}) - \frac{e^{-\frac{\beta}{T_k'} f b} \left(\frac{\alpha\beta e^{-\frac{\beta}{T_k'} f b}}{T_k'^2} - 1 \right)}{\beta b} \right)}{T_k'^2 \sigma^2 \left(e^{-\frac{\beta}{T_k'} f b} \frac{2\alpha\beta e^{-\frac{\beta}{T_k'} f b}}{T_k'^2} - 1 \right)}
\end{aligned} \tag{34}$$

$$\begin{aligned}
\frac{\partial l(\alpha, \beta, b, \sigma)}{\partial \sigma} = & \frac{2\alpha\beta e^{-\frac{\beta}{T_k'} f b} \left(X(t_j) - e^{-\frac{\beta}{T_k'} f b} X(t_{j-1}) - \frac{e^{-\frac{\beta}{T_k'} f b} \left(\frac{\alpha\beta e^{-\frac{\beta}{T_k'} f b}}{T_k'^2} - 1 \right)}{\beta b} \right)^2}{T_k'^2 \sigma^3 \left(e^{-\frac{\beta}{T_k'} f b} \frac{2\alpha\beta e^{-\frac{\beta}{T_k'} f b}}{T_k'^2} - 1 \right)} - \frac{1}{\sigma}
\end{aligned} \tag{35}$$

Appendix D. Conventional ADT model for LED reliability assessment

According to the TM-21, [5] proposes an exponential degradation model for [lumen degradation](#), as follows:

$$\phi(t) = \phi_o \cdot \exp(-\eta \cdot t) + \sigma \cdot B(t) \tag{36}$$

where,

- t : operating time in hours;
- $\phi(t)$: averaged normalized of **luminous intensity** at time t ;
- ϕ_o : projected initial constant derived by the least squares curve-fit;
- η : decay rate constant derived by the least squares curve-fit; $\eta = \alpha \cdot \exp\left(-\frac{\beta}{T_k}\right)$; where α is the pre-exponential factor, $\beta = \frac{E_a}{k_B}$, E_a is the activation energy, k_B is the Boltzmann's constant;
- $B(t)$ is a standard Brownian motion

As a special case without self-heating consideration, Si et al [29] gave a probability distribution function (PDF) of the first hitting time of a threshold value D as follows:

$$\begin{aligned}
f_{\xi}(t) &= \frac{1}{\sqrt{2\pi t}} \left(\frac{S_B^2(t)}{t} + \frac{1}{\sigma} \gamma(t, \theta) \right) \exp\left(-\frac{S_B^2(t)}{2t}\right) \\
S_B(t) &= \frac{1}{\sigma} \left(D - \int_0^t \gamma(s, \theta) ds \right) \\
\int_0^t \gamma(s, \theta) ds &= \phi_o \cdot \exp(-\eta \cdot t)
\end{aligned} \tag{37}$$

The parameter estimation of this model, $\theta = \{\alpha, \beta, \sigma\}$ was performed according to the properties of the Wiener process. We let $x_{ikj} = \phi_i(t_{kj}) - \phi_i(t_{k(j-1)})$ be a signal increment correspondence to the component which is monitored at separated times, and $\Delta t = t_j - t_{j-1}$. So,

$$\begin{aligned}
x_{ikj} &\sim N \left(\int_{t_{j-1}}^{t_j} \gamma(s, \theta) ds, \sigma^2 (t_j - t_{j-1}) \right) \\
\int_0^t \gamma(s, \theta) ds &= \phi_o \cdot \exp(-\eta \cdot t) \\
\eta &= \alpha \cdot \exp\left(-\frac{\beta}{T_k}\right)
\end{aligned} \tag{38}$$

According to Eq. (38), the likelihood function was given:

$$L(\theta) = \prod_{k=1}^K \prod_{i=1}^{n_k} \prod_{j=1}^{m_k} \frac{1}{\sqrt{2\pi\sigma^2(t_j - t_{j-1})}} e^{-\left(\frac{[x_{ikj} - \int_{t_{j-1}}^{t_j} \gamma(s, \theta) ds]^2}{2\sigma^2(t_j - t_{j-1})} \right)} \tag{39}$$

We would not try to provide mathematical proof of the feasibility of this likelihood function. The models' parameters can be obtained by integrally solving the partial derivative equations using the numerical solutions for nonlinear algebraic equation groups thanks to a MATLAB procedure.

References

- [1] J. Cho, J. H. Park, J. K. Kim, and E. F. Schubert, "White light-emitting diodes: History, progress, and future," *Laser & photonics reviews*, vol. 11, no. 2, p. 1600147, 2017.

- [2] M.-H. Chang, D. Das, P. Varde, and M. Pecht, "Light emitting diodes reliability review," *Microelectronics Reliability*, vol. 52, no. 5, pp. 762–782, 2012.
- [3] M. Fukuda, "Reliability and degradation of semiconductor lasers and leds," *Artech House*, pp. 325–333, 1991.
- [4] R. Tuttle, K. Haraguchi, M. Hodapp, J. Jiao, C. Miller, Y. Ohno, T. Pulsipher, E. Radkov, E. Richman, and D. Szombatfalvy, "Projecting long term lumen maintenance of led light source," *Illuminating Engineering Society*, 2012.
- [5] T.-R. Tsai, C.-W. Lin, Y.-L. Sung, P.-T. Chou, C.-L. Chen, and Y. Lio, "Inference from lumen degradation data under wiener diffusion process," *IEEE Transactions on Reliability*, vol. 61, no. 3, pp. 710–718, 2012.
- [6] J. Huang, D. S. Golubović, S. Koh, D. Yang, X. Li, X. Fan, and G. Zhang, "Degradation modeling of mid-power white-light leds by using wiener process," *Optics express*, vol. 23, no. 15, pp. A966–A978, 2015.
- [7] S. H. Park and J. H. Kim, "Lifetime estimation of led lamp using gamma process model," *Microelectronics Reliability*, vol. 57, pp. 71–78, 2016.
- [8] B. Sun, X. Jiang, K.-C. Yung, J. Fan, and M. G. Pecht, "A review of prognostic techniques for high-power white leds," *IEEE Transactions on Power Electronics*, vol. 32, no. 8, pp. 6338–6362, 2016.
- [9] M. S. Ibrahim, J. Fan, W. K. Yung, Z. Wu, and B. Sun, "Lumen degradation lifetime prediction for high-power white leds based on the gamma process model," *IEEE Photonics Journal*, vol. 11, no. 6, pp. 1–16, 2019.
- [10] M. S. Ibrahim, J. Fan, W. K. Yung, A. Prisacaru, W. van Driel, X. Fan, and G. Zhang, "Machine learning and digital twin driven diagnostics and prognostics of light-emitting diodes," *Laser & Photonics Reviews*, vol. 14, no. 12, p. 2000254, 2020.
- [11] W. Nelson, *Accelerated testing: statistical models, test plans, and data analysis*, vol. 257. Wiley-Interscience, 1990.
- [12] H.-L. Ke, L. Jing, J. Hao, Q. Gao, Y. Wang, X.-x. Wang, Q. Sun, and Z.-J. Xu, "Analysis of junction temperature and modification of luminous flux degradation for white leds in a thermal accelerated reliability test," *Applied optics*, vol. 55, no. 22, pp. 5909–5916, 2016.
- [13] M. Meneghini, A. Tazzoli, G. Mura, G. Meneghesso, and E. Zanoni, "A review on the physical mechanisms that limit the reliability of gan-based leds," *IEEE Transactions on Electron Devices*, vol. 57, no. 1, pp. 108–118, 2009.

- [14] L.-R. Trevisanello, M. Meneghini, G. Mura, C. Sanna, S. Buso, G. Spiazzi, M. Vanzi, G. Meneghesso, and E. Zanoni, “Thermal stability analysis of high brightness led during high temperature and electrical aging,” in *Seventh International Conference on Solid State Lighting*, vol. 6669, p. 666913, International Society for Optics and Photonics, 2007.
- [15] F. G. Della Corte, G. Pangallo, R. Carotenuto, D. Iero, G. Marra, M. Merenda, and S. Rao, “Temperature sensing characteristics and long term stability of power leds used for voltage vs. junction temperature measurements and related procedure,” *IEEE Access*, vol. 8, pp. 43057–43066, 2020.
- [16] M. Buffolo, C. De Santi, M. Meneghini, D. Rigon, G. Meneghesso, and E. Zanoni, “Long-term degradation mechanisms of mid-power leds for lighting applications,” *Microelectronics Reliability*, vol. 55, no. 9-10, pp. 1754–1758, 2015.
- [17] M.-T. Truong, L. Mendizabal, P. Do, , and B. Iung, “A novel degradation model for led reliability assessment with accelerated stress and self-heating consideration,” in *IEEE 71st Electronic Components and Technology Conference (ECTC 2021)*, Virtual Conference, June 1 - July 4, 2021.
- [18] C. E. L. D. Sheet, “Cree’s ezbright leds,” 2007.
- [19] “FLIR Systems | Imagerie thermique, vision nocturne et systèmes de caméras infrarouges | FLIR Systems.”
- [20] L. Bian and N. Gebraeel, “Stochastic framework for partially degradation systems with continuous component degradation-rate-interactions,” *Naval Research Logistics (NRL)*, vol. 61, no. 4, pp. 286–303, 2014.
- [21] R. Assaf, P. Do, S. Nefti-Meziani, and P. Scarf, “Wear rate–state interactions within a multi-component system: a study of a gearbox-accelerated life testing platform,” *Proceedings of the Institution of Mechanical Engineers, Part O: Journal of Risk and Reliability*, vol. 232, no. 4, pp. 425–434, 2018.
- [22] P. E. Protter, “Stochastic differential equations,” in *Stochastic integration and differential equations*, pp. 249–361, Springer, 2005.
- [23] M. Meneghini, N. Trivellin, K. Orita, M. Yuri, D. Ueda, E. Zanoni, and G. Meneghesso, “Analysis of the role of current, temperature, and optical power in the degradation of ingan-based laser diodes,” *IEEE transactions on electron devices*, vol. 56, no. 2, pp. 222–228, 2009.
- [24] D. Florens-Zmirou, “Approximate discrete-time schemes for statistics of diffusion processes,” *Statistics: A Journal of Theoretical and Applied Statistics*, vol. 20, no. 4, pp. 547–557, 1989.

- [25] J. M. Steele, *Stochastic calculus and financial applications*, vol. 45. Springer Science & Business Media, 2012.
- [26] J. C. Lagarias, J. A. Reeds, M. H. Wright, and P. E. Wright, “Convergence properties of the nelder–mead simplex method in low dimensions,” *SIAM Journal on optimization*, vol. 9, no. 1, pp. 112–147, 1998.
- [27] L. Jayasinghe, T. Dong, and N. Narendran, “Is the thermal resistance coefficient of high-power leds constant?,” in *Seventh international conference on solid state lighting*, vol. 6669, p. 666911, International Society for Optics and Photonics, 2007.
- [28] D. Chu, M. Touzelbaev, K. E. Goodson, S. Babin, and R. F. Pease, “Thermal conductivity measurements of thin-film resist,” *Journal of Vacuum Science & Technology B: Microelectronics and Nanometer Structures Processing, Measurement, and Phenomena*, vol. 19, no. 6, pp. 2874–2877, 2001.
- [29] X.-S. Si, W. Wang, C.-H. Hu, D.-H. Zhou, and M. G. Pecht, “Remaining useful life estimation based on a nonlinear diffusion degradation process,” *IEEE Transactions on reliability*, vol. 61, no. 1, pp. 50–67, 2012.